Hindawi
Journal of Mathematics
Volume 2022, Article ID 2715767, 10 pages
https://doi.org/10.1155/2022/2715767

Research Article

Some Novel Analytical Approximations to the (Un)damped Duffing–Mathieu Oscillators

Haifa A. Alyousef,[1] Alvaro H. Salas,[2] Sadah A. Alkhateeb,[3] and S. A. El-Tantawy[4,5]

[1]*Department of Physics, College of Science, Princess Nourah bint Abdulrahman University, P.O. Box 84428, Riyadh 11671, Saudi Arabia*
[2]*Department of Mathematics and Statistics, Universidad Nacional de Colombia, FIZMAKO Research Group, Sede Manizales, Colombia*
[3]*Mathematics Department, Faculty of Science, University of Jeddah, Jeddah, Saudi Arabia*
[4]*Department of Physics, Faculty of Science, Port Said University, Port Said 42521, Egypt*
[5]*Research Center for Physics (RCP), Department of Physics, Faculty of Science and Arts, Al-Mikhwah, Al-Baha University, Saudi Arabia*

Correspondence should be addressed to S. A. El-Tantawy; tantawy@sci.psu.edu.eg

Received 24 December 2021; Accepted 27 March 2022; Published 5 May 2022

Academic Editor: Fairouz Tchier

Some novel exact solutions and approximations to the damped Duffing–Mathieu-type oscillator with cubic nonlinearity are obtained. This work is divided into two parts: in the first part, some exact solutions to both damped and undamped Mathieu oscillators are obtained. These solutions are expressed in terms of the Mathieu functions of the first kind. In the second part, the equation of motion to the damped Duffing–Mathieu equation (dDME) is solved using some effective and highly accurate approaches. In the first approach, the nonintegrable dDME with cubic nonlinearity is reduced to the integrable dDME with linear term having undermined optimal parameter (maybe called reduced method). Using a suitable technique, we can determine the value of the optimal parameter and then an analytical approximation is obtained in terms of the Mathieu functions. In the second approach, the ansatz method is employed for deriving an analytical approximation in terms of trigonometric functions. In the third approach, the homotopy perturbation technique with the extended Krylov–Bogoliubov–Mitropolskii (HKBM) method is applied to find an analytical approximation to the dDME. Furthermore, the dDME is solved numerically using the Runge–Kutta (RK) numerical method. The comparison between the analytical and numerical approximations is carried out. All obtained approximations can help a large number of researchers interested in studying the nonlinear oscillations and waves in plasma physics and many other fields because many evolution equations related to the nonlinear waves and oscillations in a plasma can be reduced to the family of Mathieu-type equation, Duffing-type equation, etc.

1. Introduction

Several physical and natural phenomena related to biology, chemistry, physics, engineering problems, and so on can be modelled by both ordinary differential equations (ODEs) and partial differential equations (PDEs) for studying the nonlinear self-excited oscillators [1–12]. Also, in many real-life problems, some internal and external forces that can affect the system under consideration cannot be neglected. For example, the friction and collisional force and many others that affect on the motion of particles, whether in solid, liquid, gas or plasma physics, cannot be neglected. Therefore, these forces must be included in the mathematical models that will be used for studying the natural and physical problem, such as investigating the nonlinear oscillations in various plasma models [13–23]. Interest in the study of nonlinear oscillations in a plasma is due to its many potential applications. Nowadays, plasma processing is seen as an important and effective technology which has been able to enter into all modern industries. In addition, plasma had a great credit for the modern technology in electronics, medicine, agriculture, biomedicine, automobiles, optics, aerospace, telecommunications, solar energy, polymers, papers, textiles, etc. [16, 24]. Therefore, we focus our attention on the applications of the family of Duffing-type equation for modelling the nonlinear oscillations in a plasma. The Duffing-type oscillator is one of the most popular differential equations that has spread widely due to its ability to explain many nonlinear phenomena in various fields of science and in mechanical systems and engineering. This equation is a mathematical model described by a second order of ODEs with a nonlinear spring force. It is used for describing the motion of (un)damped oscillator rather than simple harmonic motion. Motivated by potential engineering and plasma physics applications in addition to many others applications in electronic circuits and microcontroller, the family of Duffing equation such as (un) damped Duffing equation with lower and higher-order nonlinearities, (un)damped Duffing–Helmholtz equation, and (un)damped Mathieu–Duffing equation have received wide attention due to their ability for investigating the mechanism of a rigid pendulum oscillator, oscillations in different plasma models, and so on. This family of second-order differential equations has provided useful and successful models for investigating the nonlinear oscillations and chaotic nature. The biggest challenge in the study of the dynamics of nonlinear mechanical systems is to find some real solutions (including the analytical and numerical solutions) to the evolution equations that are used for describing the characteristics of nonlinear phenomena under consideration. Accordingly, studying the solutions of many equations of motion to various oscillators is one of the most difficult tasks facing many researchers.

The solutions associated to mentioned evolution equations and many other related equations have been studied extensively due to the fact that such equations arise in a variety of realistic problems. For instance, the fluid equations of electron-ion unmagnetized cold plasma were reduced to Mathieu equation in order to investigate the electron waves [13]. During this study, the authors assumed that the density perturbations of the plasma species are only time-dependent functions and do not depend on space. Also, the basic set of fluid equations to a multicomponent complex plasma consisting of inertial two types of dust grains (both positive and negative charges) as well as inertialess Maxwellian species including electrons and ions were reduced to a Mathieu-type equation for studying the excitation of dust-acoustic oscillations [14]. Moreover, a nonlinear Van der Pol–Mathieu-type equation was derived for the dust grain density in order to investigate the dynamics of dust-acoustic oscillations in a dusty plasma consisting of inertial Boltzmann distributed species (electrons and ions) and inertialess dust grains [15]. A modified Van der Pol–Duffing oscillator with forced term was used in the study and was used in modelling the dynamics of nonlinear oscillations in different plasma models [16]. More recently, the multistage method was used for solving the damping Duffing equation with forced term in order to model the oscillations in a complex unmagnetized plasma [17].

Due to the importance of the family of Duffing-type equation and motivated by the mentioned studies, we focus our attention on the analysis of the so-called (un)damped Mathieu–Duffing oscillator with a twin-well potential [25].

$$\mathbb{R} \equiv \ddot{x} + \left(\alpha - Q_0 \cos(\Omega t)\right)x + \beta x^3 = 0, \tag{1}$$

and

$$\mathbb{R}_1 \equiv \ddot{x} + \varepsilon\dot{x} + \left(\alpha - Q_0 \cos(\Omega t)\right)x + \beta x^3 = 0, \tag{2}$$

for studying the vibrating/oscillating behavior of systems described by (1) and (2), where $(\alpha, \beta) > 0$ are, respectively, the stiffness coefficients of the linear and nonlinear terms and ε represents the coefficients of damping term. The longitudinal loading is periodic, Ω and Q_0 are the frequency and excitation strength of the periodic loading, respectively. The total energy of the undamped Mathieu–Duffing oscillator (DMO) according to (1) is defined by $H = H_0 + H_1$, where $H_0 = 1/2\dot{x}^2 - 1/2\alpha x^2 + 1/4\beta x^4$ and $H_1 = -1/2x^2 Q_0 \cos(\Omega t)$ are, respectively, the unperturbed and perturbation in the Hamiltonian of (1). There is another form to the equation of periodic motion which is called (un)damped Mathieu–Helmholtz oscillator.

$$\begin{cases} \ddot{x} + \left(\alpha - Q_0 \cos(\Omega t)\right)x + \beta x^2 = 0, \\ \ddot{x} + \varepsilon\dot{x} + \left(\alpha - Q_0 \cos(\Omega t)\right)x + \beta x^2 = 0. \end{cases} \tag{3}$$

The analytical solution to the damped Mathieu–Helmholtz oscillator (3) was obtained using the finite Fourier series expansion [26]. Note that in evolution equation (3), the nonlinear term βx^2 is different from the nonlinear term in equations (1) and (2).

The objectives of our study are to find some novel solutions to the (un)damped Duffing–Mathieu-type oscillator, under the initial conditions $x(0) = 0$ and $x'(0) = \dot{x}_0$. Two cases for Duffing–Mathieu-type oscillator will be discussed. In the first case, we will get some exact solutions to (un)damped Mathieu equation in terms of the Mathieu functions of the first kind. In the second case, the damped Duffing–Mathieu oscillator (dDMO) will be solved analytically and numerically using some different approaches. In the first approach, the cubic nonlinear term in equation (1) βx^3 is replaced by the linear term $\beta\kappa x$, where the constant $\kappa \geq 0$ represents an optimal parameter. Then, the nonintegrable dDMO reduces to an integrable one which has an exact solution but with undermined parameter κ. Using a suitable technique, we can determine the value of the optimal parameter κ. Thus, we can get an analytical approximation to the dDMO (2) in terms of the Mathieu functions. For the second approach, the ansatz method with the help of the solution to the undamped Duffing oscillator is employed to derive an analytical approximation to the dDMO (2) in the form of trigonometric functions. Furthermore, the homotopy perturbation technique with the extended Krylov–Bogoliubov–Mitropolskii (KBM) which is called HKBM method is also devoted for solving the dDME (2) for arbitrary physical parameters [27, 28].

2. Mathematical Analysis

Here, we proceed to find some approximate solutions to both undamped and damped Duffing–Mathieu oscillators (1) and (2), respectively. Below we discuss the different approaches for solving the mentioned equations.

2.1. An Exact Solution to (Un)damped Mathieu Equation. Both undamped Mathieu equation, i.e., (1) for $\beta = 0$, and the damped Mathieu equation, i.e., (2) for $\beta = 0$, have exact solutions in the form of Mathieu functions. First, let us find the solution of the following damped Mathieu equation:

$$\ddot{x} + \varepsilon\dot{x} + (\alpha - Q_0 \cos(\Omega t))x = 0, \tag{4}$$

with subjected to the initial conditions (ICs): $x(0) = x_0$ and $x'(0) = \dot{x}_0$.

Using the following MATHEMATICA command

$$\begin{gathered} g[t\_] := x''[t] + 2\varepsilon\, x'[t] - (\alpha - Q_0 \mathrm{Cos}[\Omega t])x[t] \\ (\mathrm{NDSolve}[g[t] == 0 \&\& x[0] == x_0 \&\& x'[0] == \dot{x}_0, x[t], t][1,1,2] // \mathrm{FullSimplify})^1, \end{gathered} \tag{5}$$

we can get the exact solution to (4) as follows:

$$x(t) = e^{-\varepsilon t}\left(\frac{x_0 MC_1(t,\varepsilon)}{MC_1(0,\varepsilon)} + \frac{2(\varepsilon x_0 + \dot{x}_0)}{\Omega}\frac{MS_1(t,\varepsilon)}{\mathrm{MathieuSPrime}\left[4\left(\alpha - \varepsilon^2\right)/\Omega^2, 2Q_0/\Omega^2, 0\right]}\right), \tag{6}$$

with

$$\begin{aligned} MC_1(t,\varepsilon) &= \mathrm{MathieuC}\left[\frac{4\left(\alpha - \varepsilon^2\right)}{\Omega^2}, \frac{2Q_0}{\Omega^2}, \frac{\Omega}{2}t\right], \\ MS_1(t,\varepsilon) &= \mathrm{MathieuS}\left[\frac{4\left(\alpha - \varepsilon^2\right)}{\Omega^2}, \frac{2Q_0}{\Omega^2}, \frac{\Omega}{2}t\right], \end{aligned} \tag{7}$$

where MathieuS and MathieuC are the Mathieu functions of the first kind or sometimes called sine-elliptic and cosine-elliptic, respectively. For $\varepsilon = 0$, the damped Mathieu equation (4) reduces to the following undamped Mathieu equation:

$$\ddot{x} - (\alpha + Q_0 \cos(\Omega t))x = 0, \tag{8}$$

and solution (6) reduces to the following one:

$$x(t) = \frac{x_0 MC_1(t,0)}{MC_1(0,0)} + \frac{2\dot{x}_0 MS_1(t,0)}{\Omega \mathrm{MathieuSPrime}\left[4\alpha/\Omega^2, 2Q_0/\Omega^2, 0\right]}. \tag{9}$$

The exact solution (6) is compared with RK numerical solution as shown in Figures 1(a) and 1(b) for different values of x_0.

2.2. Some Analytical Approximations to the Damped Duffing–Mathieu Oscillator. Here, we proceed to discuss two techniques (the hybrid p–expansion method and the ansatz method) for finding some analytical approximations to dDMO (2). For studying dDMO (2), first we rewrite equation (2) in the following new i.v.p.

$$\begin{cases} \mathbb{R}_1 = 0, \\ x(0) = x_0 \,\&\, x'(0) = \dot{x}_0. \end{cases} \tag{10}$$

2.2.1. First Approach: Reduced Method. For $\beta \neq 0$ and $\alpha > 0$, we may obtain simple approximation to the i.v.p. (10) by replacing the cubic term βx^3 by the linear term $\beta\kappa x$, where the constant $\kappa \geq 0$ which is used as an optimal parameter to reduce the residual error. Accordingly, dDMO (2) of cubic nonlinearity reduces to the following dDMO with linear term. Thus, we can replace the i.v.p. (10) by the following new i.v.p.

$$\begin{cases} \ddot{x} + 2\varepsilon\dot{x} + (\alpha - Q_0 \cos(\Omega t))x + \beta\kappa x = 0, \\ x(0) = x_0 \text{ and } x'(0) = \dot{x}_0. \end{cases} \tag{11}$$

Thus, the exact solution to the i.v.p. (11) is expressed by

$$x_\kappa \equiv x_\kappa(t) = e^{-\varepsilon t}\left(\frac{x_0 MC_2(t,\varepsilon,\kappa)}{MC_2(0,\varepsilon,\kappa)} + \frac{2(\varepsilon x_0 + \dot{x}_0)}{\Omega}\frac{MS_2(t,\varepsilon,\kappa)}{\mathrm{MathieuSPrime}\left[4\left(\beta\kappa - \varepsilon^2 + \alpha\right)/\Omega^2, 2Q_0/\Omega^2, 0\right]}\right), \tag{12}$$

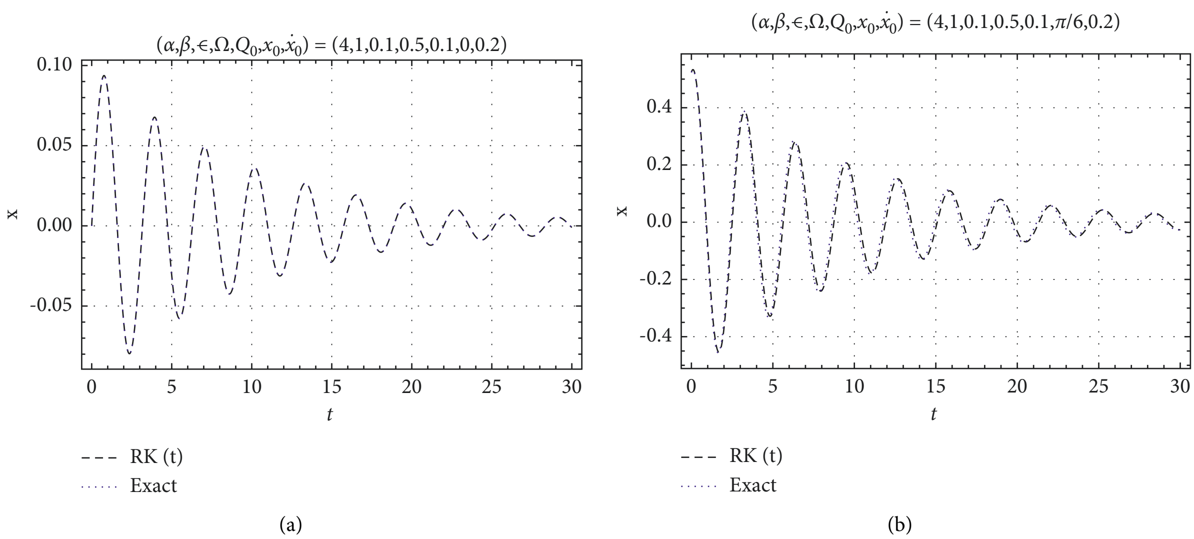

Figure 1: Both exact solution (6) and RK numerical solution to the damped Mathieu equation (4) are compared with each other for different values to the initial amplitude x_0.

with

$$MC_2(t,\varepsilon,\kappa) = \mathrm{MathieuC}\left[\frac{4(\beta\kappa-\varepsilon^2+\alpha)}{\Omega^2},\frac{2Q_0}{\Omega^2},\frac{\Omega}{2}t\right],$$
$$MS_2(t,\varepsilon,\kappa) = \mathrm{MathieuS}\left[\frac{4(\beta\kappa-\varepsilon^2+\alpha)}{\Omega^2},\frac{2Q_0}{\Omega^2},\frac{\Omega}{2}t\right]. \tag{13}$$

The residual is defined as

$$R_\kappa(t) = \ddot{x}_\kappa + \varepsilon\dot{x}_\kappa + (\alpha - Q_0\cos(\Omega t))x_\kappa + \beta x_\kappa^3. \tag{14}$$

A suitable value of κ can be obtained by solving the equation $R_\kappa(t_0)=0$ for some $t_0>0$, say $t_0=1$. Making use of the Padé approximate technique, for $0<t_0\le 1$ and $x_0\approx 0$, we get

$$\kappa_{\mathrm{suitable}} = \frac{Y_1}{Y_2}, \tag{15}$$

with

$$\begin{aligned}Y_1 ={}& 3x_0^2\left(Q_0t_0x_0^2-\alpha t_0x_0^2-2\varepsilon t_0\dot{x}_0x_0-4t_0\dot{x}_0^2-2\dot{x}_0x_0\right)\\&\times\left(4Q_0t_0x_0^2-4\alpha t_0x_0^2+3\beta t_0x_0^4-8\varepsilon t_0\dot{x}_0x_0-6t_0\dot{x}_0^2-8\dot{x}_0x_0\right),\\Y_2 ={}& -26\alpha Q_0t_0^2x_0^4+12\beta Q_0t_0^2x_0^6-52\varepsilon Q_0t_0^2\dot{x}_0x_0^3+13Q_0^2t_0^2x_0^4\\&-52Q_0t_0\dot{x}_0x_0^3-30Q_0t_0^2\dot{x}_0^2x_0^2+13\alpha^2t_0^2x_0^4-12\alpha\beta t_0^2x_0^6\\&+52\alpha\varepsilon t_0^2\dot{x}_0x_0^3+52\alpha t_0\dot{x}_0x_0^3+30\alpha t_0^2\dot{x}_0^2x_0^2+9\beta^2t_0^2x_0^8\\&-24\beta\varepsilon t_0^2\dot{x}_0x_0^5-24\beta t_0\dot{x}_0x_0^5+12\beta t_0^2\dot{x}_0^2x_0^4+52\varepsilon^2t_0^2\dot{x}_0^2x_0^2\\&+104\varepsilon t_0\dot{x}_0^2x_0^2+60\varepsilon t_0^2\dot{x}_0^3x_0+60t_0\dot{x}_0^3x_0+12t_0^2\dot{x}_0^4+52\dot{x}_0^2x_0^2.\end{aligned} \tag{16}$$

For a given κ, the residual error $L_R(\kappa)$ of the approximation (12) to the i.v.p. (10) is defined as

$$L_R(\kappa) = \max_{0\le t\le T}\left|R_\kappa(t)\right| = \max_{0\le t\le T}\left|\ddot{x}_\kappa + 2\varepsilon\dot{x}_\kappa + (\alpha - Q_0\cos(\Omega t))x_\kappa + \beta x_\kappa^3\right|. \tag{17}$$

The optimal value of $\kappa_{\mathrm{optimal}}$ for the parameter κ on the interval $0\le t\le T$ is defined as

$$\kappa_{\mathrm{optimal}} = \min_{\kappa\ge 0} L_R(\kappa). \tag{18}$$

Let us apply the obtained approximation (12) for investigating the properties of the damping oscillations to the dDMO (2) at different values to the physical parameters $(\alpha,\beta,\varepsilon,\Omega,Q_0,x_0,\dot{x}_0)$. The profile of the approximation (12) using the values of $\kappa_{\mathrm{suitable}}$ (given in equation (15)) and $\kappa_{\mathrm{optimal}}$ (given in (18)) is displayed in Figures 2 and 3 at $(\alpha,\beta,\varepsilon,\Omega,Q_0,x_0,\dot{x}_0) = (4,1,0.1,0.5,0.1,0,0.2)$ and $(\alpha,\beta,\varepsilon,\Omega,Q_0,x_0,\dot{x}_0) = (4,1,0.1,0.5,0.1,\pi/6,0.2)$, respectively. The obtained results showed that this approximation gives results with good and acceptable accuracy.

2.2.2. The Ansatz Method for Solving dDMO. Now, we can summarize the main points to get some approximations to the i.v.p. (10) in the following steps.

Step 1. Let us assume the following ansatz:

$$x(t) = y(f(t)), \tag{19}$$

where the time-dependent function $f\equiv f(t)$ can be determined later and the function $y\equiv y(t)$ represents the solution of the following i.v.p.

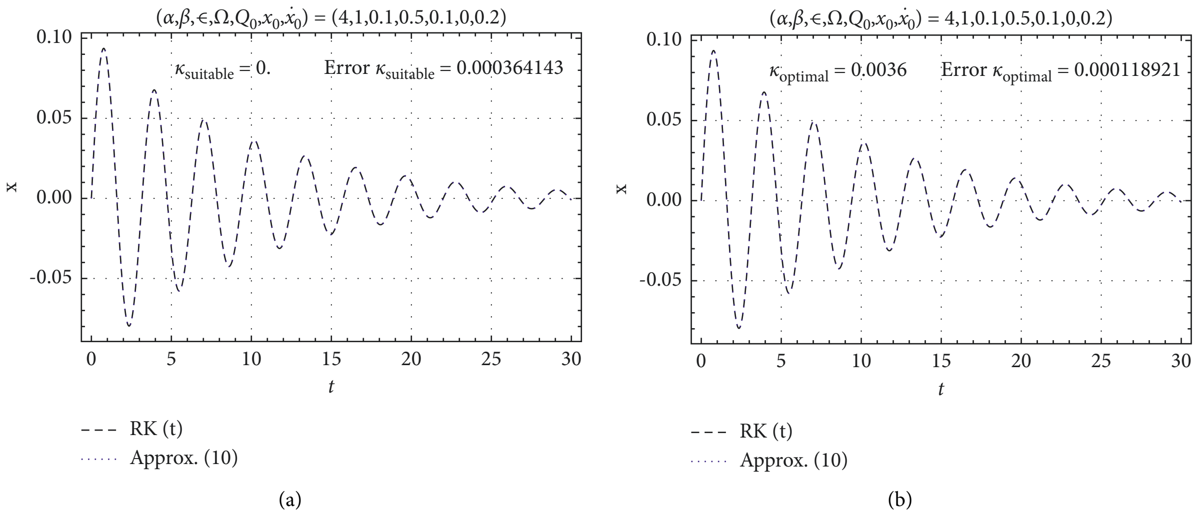

Figure 2: The profile of the approximation (12) using the values of κ_{suitable} (given in equation (15)) and κ_{optimal} (given in (18)) is plotted against t for $(\alpha, \beta, \varepsilon, \Omega, Q_0, x_0, \dot{x}_0) = (4, 1, 0.1, 0.5, 0.1, 0, 0.2)$.

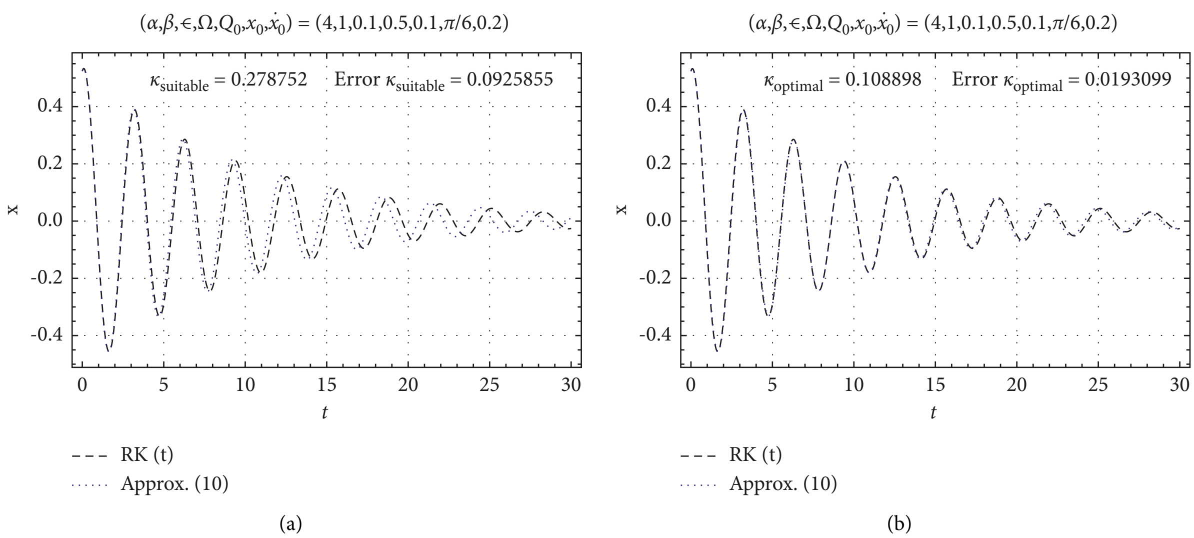

Figure 3: The profile of the approximation (12) using the values of κ_{suitable} (given in equation (15)) and κ_{optimal} (given in (18)) is plotted against t for $(\alpha, \beta, \varepsilon, \Omega, Q_0, x_0, \dot{x}_0) = (4, 1, 0.1, 0.5, 0.1, \pi/6, 0.2)$.

$$\left\{ \ddot{y} + 2\varepsilon \dot{y} + (\alpha - Q_0) y + \beta y^3 = 0,\ y(0) = x_0 \,\&\, y'(0) = \dot{x}_0. \right. \tag{20}$$

Step 2. Inserting ansatz (19) into i.v.p. (10), we get

$$\begin{aligned} \mathbb{R}_1 = {} & y'(f)\left(-2\varepsilon f'^2 + 2\varepsilon f' + f''\right) \\ & + y(f)\left(\alpha - Q_0 \cos(\Omega t) + f'^2 (Q_0 - \alpha)\right) \\ & + \beta y^3(f)\left(1 - f'^2\right). \end{aligned} \tag{21}$$

Step 3. For vanishing the coefficient of $y(f)$ in equation (21), we get

$$f'^2 = \frac{-\alpha + Q_0 \cos(\Omega t)}{(Q_0 - \alpha)}. \tag{22}$$

Step 4. Integrating equation (22) and with the help of $f(0) = 0$, we have

$$f(t) = \frac{2}{\Omega} E\left(\frac{\Omega}{2} t, \frac{2Q_0}{Q_0 - \alpha}\right), \tag{23}$$

where E stands for the EllipticE function.

Now, the value of $f(t)$ has been determined but the solution of the i.v.p. (20) needs to be determined. Thus, we are faced with two things: either we use one of the solutions found in the literature [29] or try to find another solution in the form of trigonometric functions.

Step 5. In this step, we proceed to find a solution to i.v.p. (20) in the form of trigonometric functions. Without loss of generality, i.v.p. (20) can be redefined as

$$\begin{cases} \mathbb{R}_2 = \ddot{v} + 2\varepsilon\dot{v} + pv + qv^3 = 0, \\ v(0) = v_0 \& v'(0) = \dot{v}_0, \end{cases} \quad (24)$$

where i.v.p. (24) is the same as i.v.p. (20) with $p = (\alpha - Q_0)$, $q = \beta$, and $v(t) = y(t)$.

Step 6. Our objective here is to derive another solution that does not involve elliptic functions but an elementary solution. To do that, we assume $\varepsilon > 0$, and for $\lim_{t\longrightarrow\infty} v(t) = 0$, we get

$$v(t) = c_0 e^{-\rho t} \cos\left(h(t) + \arccos\left(\frac{x_0}{c_0}\right)\right), \quad (25)$$

where $h(0) = 0$ and $h(t)$ is undermined function.

Step 7. By substituting solution (25) into i.v.p. (24), we have

$$\begin{aligned} \mathbb{R}_2 &= c_0 \sin(\theta) e^{-\rho t}\left(-2\varepsilon h' + 2\rho h' - h''\right) + \frac{1}{4} c_0^3 q \cos(3\theta) e^{-3\rho t} \\ &\quad + \frac{1}{4} c_0 \cos(\theta) e^{-3\rho t}\left[3c_0^2 q + 4e^{2\rho t}\left(-2\varepsilon\rho - h'^2 + p + \rho^2\right)\right]. \end{aligned} \quad (26)$$

Step 8. For vanishing the coefficient of $\cos(\theta)$ in equation (26): $3c_0^2 q + 4e^{2\rho t}(-2\varepsilon\rho - h'^2 + p + \rho^2) = 0$, we have

$$h' = \pm\frac{1}{2}\sqrt{4p - 8\varepsilon\rho + 4\rho^2 + 3c_0^2 q e^{-2\rho t}}, \quad (27)$$

and by solving (27) with $h(0) = 0$, we get

$$h(t) = H(t) - H(0), \quad (28)$$

with

$$\begin{aligned} H(t) &= \frac{1}{\rho}\left(\sqrt{\Pi}\tanh^{-1}\left(\sqrt{1 + \frac{3c_0^2 q e^{-2\rho t}}{4\Pi}}\right) - \sqrt{\frac{3}{4}c_0^2 q e^{-2\rho t} + \Pi}\right), \\ H(0) &= \frac{1}{\rho}\left(\sqrt{\Pi}\tanh^{-1}\left(\sqrt{1 + \frac{3c_0^2 q}{4\Pi}}\right) - \sqrt{\frac{3}{4}c_0^2 q + \Pi}\right), \end{aligned} \quad (29)$$

where $\Pi = (p - 2\varepsilon\rho + \rho^2)$.

Step 9. The number c_0 is obtained from the condition $v'(0) = \dot{v}_0$ and it is a solution to the quartic

$$\begin{aligned} &3qc_0^4 + \left(4p - 8\varepsilon\rho + 4\rho^2 - 3qv_0^2\right)c_0^2 - 4\left(pv_0^2 - 2\varepsilon\rho v_0^2\right. \\ &\quad \left. + 2\rho^2 v_0^2 + 2\rho v_0 \dot{v}_0 + \dot{v}_0^2\right) = 0, \end{aligned} \quad (30)$$

where the number ρ is a free/optimal parameter that is chosen in order to minimize the residual error. Its default value is $\rho = \varepsilon$.

Step 10. Finally, the trigonometric approximation to i.v.p. (10) is obtained:

$$x(t) = y(f(t)) = c_0 e^{-\rho f(t)} \cos\left(h(f(t)) + \arccos\left(\frac{x_0}{c_0}\right)\right). \quad (31)$$

Step 11. Also, we can solve i.v.p. (20) using RK numerical method and then replacing $t \longrightarrow f(t)$ (given in equation (23)). The following MATHEMATICA command is introduced for this purpose:

$$\begin{aligned} &g[t\_] := y''[t] + 2\,\varepsilon\, y'[t] + (\alpha - Q_0)\, y[t] + \beta\, y[t]^3; \\ &RK[t\_] := \text{NDSolve}\left[g[t] == 0 \&\& y[0] == x_0 \&\& y'[0] \right. \\ &\qquad \left. == \dot{x}_0, y[t], t\right][1, 1, 2], \end{aligned} \quad (32)$$

$$x[t\_] := RK[f[t]]. \quad (33)$$

Both analytical and numerical approximations (31) and (33) to i.v.p. (10) are, respectively, plotted against the RK numerical solution as illustrated in Figures 4 and 5. Also, at $(\alpha, \beta, \varepsilon, \Omega, Q_0, \dot{x}_0) = (4, 1, 0.1, 0.5, 0.1, 0.2)$, the maximum global distance of both approximations (31) and (33) is estimated for different values to x_0 as

$$\begin{aligned} L_d(x_0 = 0) &= \max_{0\le t\le 30}\left|RK - x(t)_{\text{Approx. (26)}}\right| = 0.000506901, \\ L_d(x_0 = 0) &= \max_{0\le t\le 30}\left|RK - x(t)_{\text{Approx. (28)}}\right| = 0.000482946, \\ L_d\left(x_0 = \frac{\pi}{6}\right) &= \max_{0\le t\le 30}\left|RK - x(t)_{\text{Approx. (26)}}\right| = 0.00415468, \\ L_d\left(x_0 = \frac{\pi}{6}\right) &= \max_{0\le t\le 30}\left|RK - x(t)_{\text{Approx. (28)}}\right| = 0.00266014. \end{aligned} \quad (34)$$

The obtained results show the high accuracy and efficiency of the obtained approximations (31) and (33). Moreover, these approximations are stable against long time and for arbitrary values of the physical parameters.

2.3. The Homotopy Extended Krylov–Bogoliubov–Mitropolskii Method.

The homotopy extended Krylov–Bogoliubov–Mitropolskii (HKBM) method may be used for solving both conservative and nonconservative oscillators. Based on this method (more details can be found in [27, 28]), i.v.p. (10) can be redefined as

$$\begin{cases} \ddot{x} + (\alpha - Q_0)x + p\left[\varepsilon\dot{x} + Q_0(1 - \cos(\Omega t))x + \beta x^3\right] = 0, \\ x(0) = x_0 \text{ and } x'(0) = \dot{x}_0, 0 \le t \le T, \end{cases} \quad (35)$$

where $x_p \equiv x_p(t)$ indicates the solution of i.v.p. (35) while the solution of the dDMO (2) is obtained for $p = 1$. For $\omega_0 = \sqrt{\alpha - Q_0}$, $\phi(t) = Q_0(1 - \cos(\Omega t))$ and $\alpha - Q_0 > 0$, i.v.p. (35) can be written in the following reduced form:

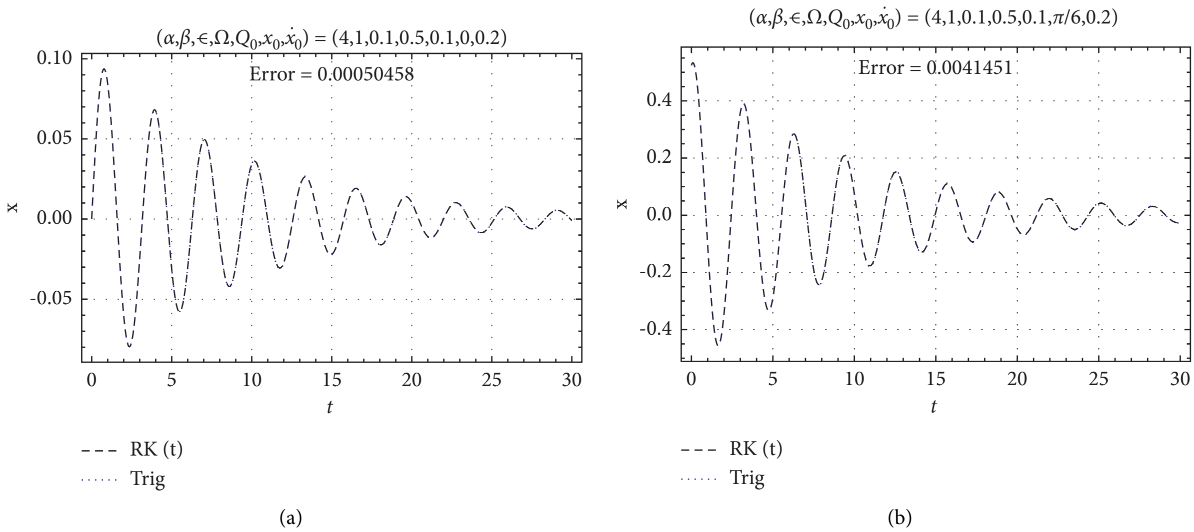

Figure 4: Both trigonometric approximation (31) and RK numerical simulation to the damped Duffing–Mathieu problem (10) are compared with each other for different values to the initial amplitude x_0.

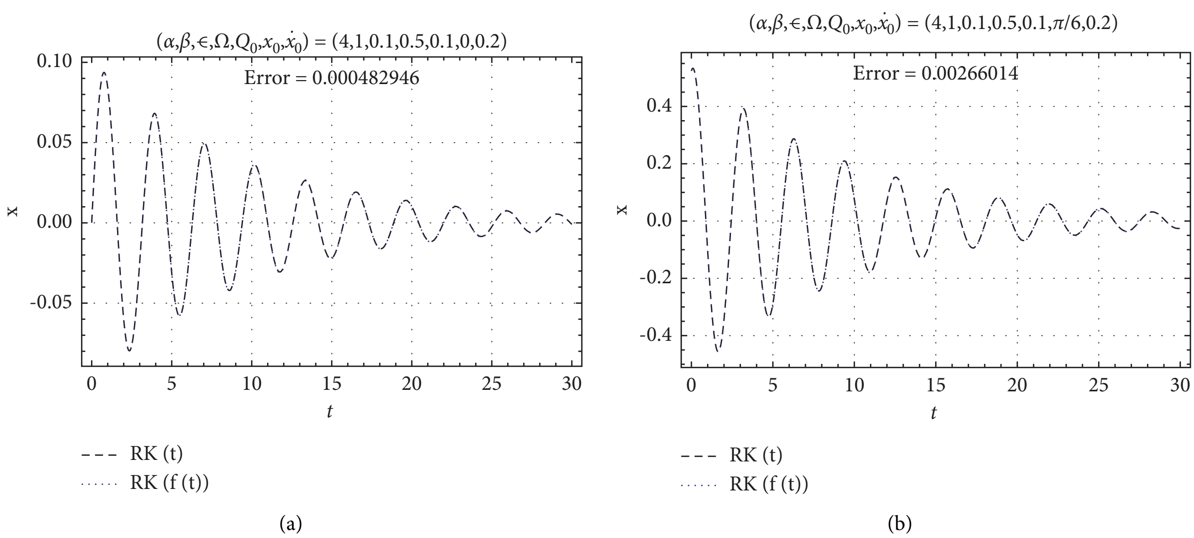

Figure 5: Both RK numerical simulation (32) and RK numerical simulation (33) using the definition of $t \longrightarrow f(t)$ to the damped Duffing–Mathieu problem (10) are compared with each other for different values to the initial amplitude x_0.

$$\begin{cases} \ddot{x} + \omega_0^2 x + p\left(\varepsilon\dot{x} + \phi(t)x + \beta x^3\right) = 0, \\ x(0) = x_0 \text{ and } x'(0) = \dot{x}_0, 0 \le t \le T. \end{cases} \tag{36}$$

According to the HKBM method, the following ansatz solution is introduced:

$$x_p = a\cos(\psi) + \sum_{n=1}^{N} p^n u_n(a,\psi) + O\left(p^{N+1}\right), \tag{37}$$

where each $u_n \equiv u_n(a,\psi)$ is a periodic function in ψ, and both amplitude a and phase ψ are assumed to vary with time and subject to the conditions

$$\begin{aligned} \frac{da}{dt} &\equiv \dot{a} = \sum_{n=1}^{N} p^n A_n(a) + O\left(p^{N+1}\right), \\ \frac{d\psi}{dt} &\equiv \dot{\psi} = \omega_0 + \sum_{n=1}^{N} p^n \psi_n(a) + O\left(p^{N+1}\right), \end{aligned} \tag{38}$$

where $a \equiv a(t)$ and $\psi \equiv \psi(t)$.

Inserting ansatz solution (37) and using (38) and after several tedious calculations, we can determine the unknown time-dependent functions (u_n, ψ_n, A_n, a). To avoid the so-called secularity, we choose only the solution that does not contain cos ψ nor sin ψ. For $N = 1$, we get

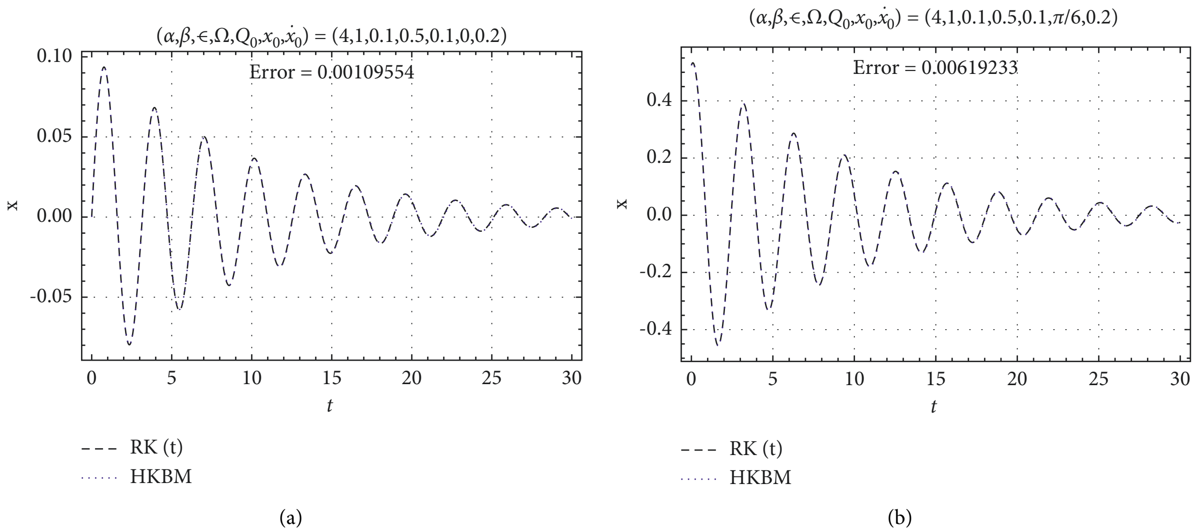

Figure 6: Both HKBM first-order approximate solution (42) and RK numerical simulation are plotted against different values of the initial angle x_0.

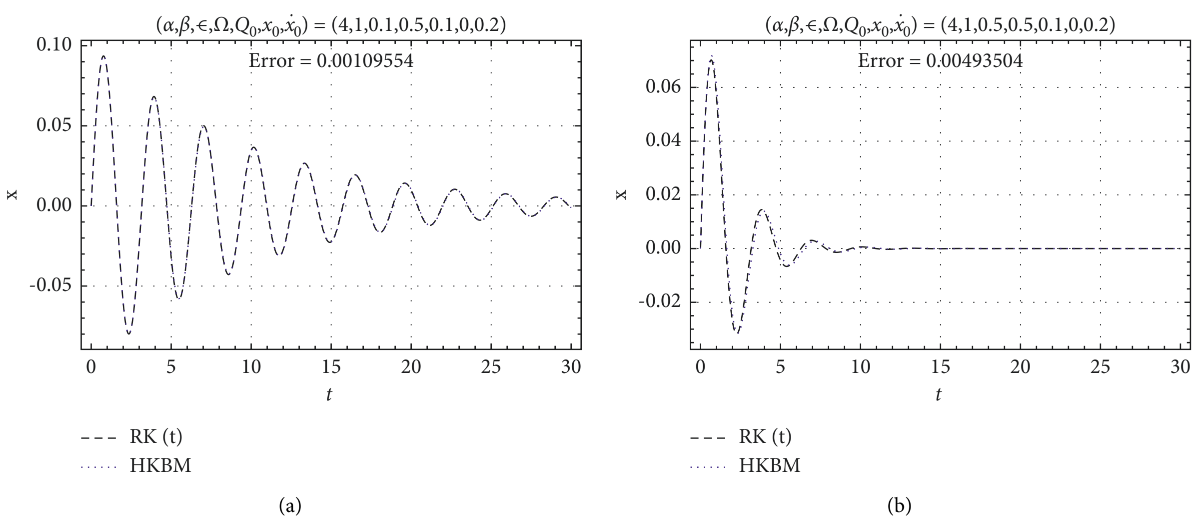

Figure 7: Both HKBM first-order approximate solution (42) and RK numerical simulation are plotted against different values of the damping parameter ε.

$$\begin{aligned} \dot{a} &= -\varepsilon a(t), \\ \dot{\psi} &= \frac{3\beta a(t)^2 + 4\phi(t)}{8\omega_0} + \omega_0, \\ u_1(a,\psi) &= \frac{a^3\beta\cos(3\psi)}{32\omega_0^2}, \end{aligned} \tag{39}$$

and

$$x_p(t) = a\cos(\psi) + p\frac{\beta}{32\omega_0^2}a^3\cos(3\psi). \tag{40}$$

By solving system (39), we have

$$\begin{aligned} a &= c_0 e^{-\varepsilon t}, \\ \psi &= \frac{e^{-2\varepsilon t}}{16\varepsilon\Omega\omega_0}\left[8\varepsilon e^{2\varepsilon t}\left(2c_1\Omega\omega_0 - Q_0(\Omega t + \sin(\Omega t)) + 2\alpha\Omega t\right)\right. \\ &\quad \left. + 3\beta c_0^2\Omega\left(e^{2\varepsilon t} - 1\right)\right]. \end{aligned} \tag{41}$$

The first-order approximate solution is obtained for $p = 1$:

$$x(t) = x_1(t) = a\cos(\psi) + \frac{\beta}{32\omega_0^2}a^3\cos(3\psi), \tag{42}$$

where the values of (a, ψ) are defined in (41) while the constants c_0 and c_1 can be obtained from the initial conditions.

The comparison between the HKBM first-order approximate solution (37) and the RK numerical simulation is reported as shown in Figures 6(a) and 6(b) for $x_0 = 0$ and $x_0 = \pi/6$, respectively. Also, both HKBM first-order approximate solution (42) and RK numerical simulation are, respectively, compared with each other for weak $(\varepsilon = 0.1)$ and strong $(\varepsilon = 0.5)$ damping as illustrated in Figures 7(a) and 7(b). Furthermore, at $(\alpha, \beta, \Omega, Q_0, \dot{x}_0) = (4, 1, 0.5, 0.1, 0.2)$ and for different values to (x_0, ε), the maximum global distance error to the HKBM first-order approximate solution (42) is estimated as

$$
\begin{aligned}
L_d(x_0 = 0) &= \max_{0 \le t \le 30} \left| RK - x(t)_{\mathrm{HKBM}(37)} \right| = 0.00110165, \\
L_d\left(x_0 = \frac{\pi}{6}\right) &= \max_{0 \le t \le 30} \left| RK - x(t)_{\mathrm{HKBM}(37)} \right| = 0.0061929, \\
L_d(\varepsilon = 0.1) &= \max_{0 \le t \le 30} \left| RK - x(t)_{\mathrm{HKBM}(37)} \right| = 0.00110165, \\
L_d(\varepsilon = 0.5) &= \max_{0 \le t \le 30} \left| RK - x(t)_{\mathrm{HKBM}(37)} \right| = 0.00493896.
\end{aligned} \tag{43}
$$

It is clear that the HKBM first-order approximate solution (42) is characterized by high accuracy and more stability at long time.

3. Conclusion

Given the importance of nonlinear oscillations in plasma physics and engineering and their strong connection to the family of the Duffing-type oscillator, in this work, some exact solutions to the damped and undamped Mathieu equations as well as some analytical approximations to the damped Duffing–Mathieu oscillator (dDMO) using different approaches have been obtained. The exact solutions to both damped and undamped Mathieu equation have been obtained in the terms of Mathieu functions of the first kind. These solutions are numerically compared with the Runge–Kutta (RK) numerical simulation. It was observed that both exact and numerical solutions are completely matched with each other in the whole time interval. On the other hand, the dDMO has been solved using some different approaches. In the first one, the nonintegrable dDMO with cubic nonlinear term (βx^3) has been reduced to an integrable dDMO with linear term $(\beta \kappa x)$ in which κ is undermined optimal parameter. The kappa optimal parameter κ has been determined using a suitable technique as we discussed in the text above. After determining the kappa optimal parameter, a highly accurate analytical approximation has been obtained in terms of the Mathieu functions. In the second approach, a highly accurate analytical approximation has been derived in detail in terms of trigonometric functions using the ansatz method. In the third technique, the homotopy extended Krylov–Bogoliubov–Mitropolskii (HKBM) method was used for getting an effective analytical approximation. Furthermore, the dDMO has been analyzed numerically using the RK numerical method. The comparison between all obtained approximations and the RK numerical solutions has been carried out. Moreover, the maximum global distance error in the whole time interval to all obtained approximations has been estimated. All obtained approximations are characterized by the high accuracy and efficiency in addition to being more stable for a long time.

3.1. Future Work

We may solve the following oscillators using of the methods described in this paper:

3.1.1. Future Idea I. Cubic-quintic Duffing–Mathieu equation:

$$
\begin{cases} \ddot{x} + \omega_0^2 x + 2\varepsilon \dot{x} + \phi(t) x + \beta x^3 + \gamma x^5 = 0, \\ x(0) = x_0 \,\&\, x'(0) = x_0, \quad 0 \le t \le T. \end{cases} \tag{44}
$$

3.1.2. Future Idea II. Forced damped Duffing–Mathieu equation:

$$
\begin{cases} \ddot{x} + \omega_0^2 x + 2\varepsilon \dot{x} + \phi(t) x + \beta x^3 = F(t), \\ x(0) = x_0 \,\&\, x'(0) = x_0, \quad 0 \le t \le T. \end{cases} \tag{45}
$$

3.1.3. Future Idea III. The forced Van der Pol–Duffing oscillator:

$$
\begin{cases} \ddot{x} - \varepsilon\left(1 - x^2\right) \dot{x} + \omega_0^2 x + \beta x^3 = F(t), \\ x(0) = x_0 \,\&\, x'(0) = x_0, \quad 0 \le t \le T, \end{cases} \tag{46}
$$

and many others oscillators.

Data Availability

The data generated or analyzed during this study are included within the article.

Conflicts of Interest

The authors declare that they have no conflicts of interest.

Authors' Contributions

All authors contributed equally to this study and approved the final version of the manuscript.

Acknowledgments

The authors express their gratitude to Princess Nourah bint Abdulrahman University Researchers Supporting Project (grant no. PNURSP2022R17), Princess Nourah bint Abdulrahman University, Riyadh, Saudi Arabia.

References

[1] A.-M. Wazwaz, *Partial Differential Equations and Solitary Waves Theory*, Springer, Berlin, Germany, 2009.

[2] A.-M. Wazwaz, *Partial Differential Equations: Methods and Applications*, A.A.Balkema Publishers, Avereest, Netherlands, 2002.

[3] S. A. Almutlak and S. A. El-Tantawy, "On the approximate solutions of a damped nonplanar modified Korteweg-de Vries equation for studying dissipative cylindrical and spherical solitons in plasmas," *Results in Physics*, vol. 23, Article ID 104034, 2021.

[4] W. Albalawi, A. H. Salas, S. A. El-Tantawy, and A. A. A.-R. Youssef, "Approximate analytical and numerical solutions to the damped pendulum oscillator: Newton-Raphson and moving boundary methods," *Journal of Taibah University for Science*, vol. 15, no. 1, pp. 479–485, 2021.

[5] N. H. Aljahdaly, S. A. El-Tantawy, A.-M. Wazwaz, and H. A. Ashi, "Adomian decomposition method for modelling the dissipative higher-order rogue waves in a superthermal collisional plasma," *Journal of Taibah University for Science*, vol. 15, no. 1, pp. 971–983, 2021.

[6] S. Rajasekar, S. Parthasarathy, and M. Lakshmanan, "Prediction of horseshoe chaos in BVP and DVP oscillators," *Chaos, Solitons & Fractals*, vol. 2, no. 3, pp. 271–280, 1992.

[7] K. Johannessen, "An analytical solution to the equation of motion for the damped nonlinear pendulum," *European Journal of Physics*, vol. 35, no. 3, Article ID 035014, 2014.

[8] E. Esmailzadeh and G. Nakhaie-jazar, "Periodic solution of a Mathieu-Duffing type equation," *International Journal of Non-linear Mechanics*, vol. 32, no. 5, pp. 905–912, 1997.

[9] M. Zamora, "A note on the periodic solutions of a Mathieu–Duffing type equations," *Mathematische Nachrichten*, vol. 290, 2016.

[10] V. Belovodskiy, "About the new periodic solutions of the mathieu-duffing equation in the principal zone of instability," *Mechanics*, vol. 33, pp. 38–42, 2010.

[11] E. Babilio, "The duffing-mathieu equation arising from dynamics of post-buckled beams," *Nonlinear Dynamics of Structures, Systems and Devices*, Springer, Berlin, Germany, pp. 267–275, 2020.

[12] A. Y. T. Leung, Z. Guo, and H. X. Yang, "Transition curves and bifurcations of a class of fractional mathieu-type equations," *International Journal of Bifurcation and Chaos*, vol. 22, no. 11, Article ID 1250275, 2012.

[13] G. Brodin and L. Stenflo, "A simple electron plasma wave," *Physics Letters A*, vol. 381, no. 11, pp. 1033–1035, 2017.

[14] I. Kourakis, M. Momeni, and P. K. Shukla, "A Mathieu equation for dust charge dynamics in multi-component dusty plasmas," in *Proceedings of the 33rd EPS Conference*, vol. 30I, Rome, Italy, June 2006.

[15] M. Momeni, I. Kourakis, M. Moslehi-Fard, and P. K. Shukla, "A Van der Pol-Mathieu equation for the dynamics of dust grain charge in dusty plasmas," *Journal of Physics A: Mathematical and Theoretical*, vol. 40, no. 24, pp. F473–F481, 2007.

[16] C. H. Miwadinou, L. A. Hinviy, A. V. Monwanouz, and J. B. Chabi Orou, "Nonlinear dynamics of plasma oscillations modeled by a forced modified Van der Pol-Duffing oscillator," 2013, http://arxiv.org/abs/1308.6132v1.

[17] N. H. Aljahdaly and S. A. El-Tantawy, "On the multistage differential transformation method for analyzing damping duffing oscillator and its applications to plasma physics," *Mathematics*, vol. 9, no. 4, p. 432, 2021.

[18] A. H. Salas, S. A. El-Tantawy, and E. Jairo, "On the approximate and analytical solutions to the fifth-order Duffing oscillator and its physical applications," *Waves in Random and Complex Media*, pp. 1–21, 2021.

[19] A. H. Salas S, S. A. El-Tantawy, and M. R. Alharthi, "Novel solutions to the (un)damped Helmholtz-Duffing oscillator and its application to plasma physics: moving boundary method," *Physica Scripta*, vol. 96, no. 10, Article ID 104003, 2021.

[20] S. A. El-Tantawy, A. H. Salas, and M. R. Alharthi, "On the analytical and numerical solutions of the damped nonplanar Shamel Korteweg-de Vries Burgers equation for modeling nonlinear structures in strongly coupled dusty plasmas: multistage homotopy perturbation method," *Physics of Fluids*, vol. 33, no. 4, Article ID 043106, 2021.

[21] S. A. El-Tantawy, A. H. Salas, and M. R. Alharthi, "On the analytical solutions of the forced damping duffing equation in the form of weierstrass elliptic function and its applications," *Mathematical Problems in Engineering*, vol. 2021, Article ID 6678102, 9 pages, 2021.

[22] S. A. El-Tantawy, A. H. Salas, and M. R. Alharthi, "A new approach for modelling the damped Helmholtz oscillator: applications to plasma physics and electronic circuits," *Communications in Theoretical Physics*, vol. 73, no. 3, Article ID 035501, 2021.

[23] A. H. Salas, S. A. El-Tantawy, and N. H. Aljahdaly, "An exact solution to the quadratic damping strong nonlinearity duffing oscillator," *Mathematical Problems in Engineering*, vol. 2021, Article ID 8875589, 8 pages, 2021.

[24] J. Proud, *Plasma Processing of Materials: Scientific Opportunities and Technologies Challenges*, National Academy Press, Washington, DC, USA, 1991.

[25] A. C. J. Luo, "Chaotic motion in the generic separatrix band of a Mathieu-Duffing oscillator with a twin-well potential," *Journal of Sound and Vibration*, vol. 248, no. 3, pp. 521–532, 2001.

[26] A. C. J. Luo and B. Yu, "Analytical periodic motions of a parametric oscillator with quadratic nonlinearity," in *Proceedings of the 26th Conference on Mechanical Vibration and Noise*, Buffalo, NY, USA, August 2014.

[27] M. A. Uddin, M. W. Ullah, and R. S. Bipasha, "An approximate analytical technique for solving second order strongly nonlinear generalized duffing equation with small damping," *Journal of Bangladesh Academy of Sciences*, vol. 39, no. 1, pp. 103–114, 2015.

[28] A. H. Salas, "Analytical approximant to a quadratically damped duffing oscillator," *The Scientific World Journal*, vol. 2022, Article ID 3131253, 10 pages, 2022.

[29] A. H. Salas and S. A. El-Tantawy, "On the approximate solutions to a damped harmonic oscillator with higher-order nonlinearities and its application to plasma physics: semi-analytical solution and moving boundary method," *The European Physical Journal Plus*, vol. 135, no. 10, p. 833, 2020.